Journal of Alloys and Compounds 506 (2010) 125–130

Contents lists available at ScienceDirect

Journal of Alloys and Compounds

journal homepage: www.elsevier.com/locate/jallcom

Phase equilibria of the Zn–Bi–Ni system at 600 °C and 750 °C

Chen Xu, Fucheng Yin*, Manxiu Zhao, Yongxiong Liu, Xuping Su

Key Laboratory of Materials Design and Preparation Technology of Hunan Province, School of Mechanical Engineering, Xiangtan University, Xiangtan 411105, Hunan, PR China

ARTICLE INFO

Article history:
Received 31 May 2010
Accepted 24 June 2010
Available online 3 July 2010

Keywords:
Zn–Bi–Ni system
Phase diagram
Scanning electron microscope
Zn-based alloy

ABSTRACT

The 600 °C and 750 °C isothermal sections of the Zn–Bi–Ni ternary system have been determined experimentally using scanning electron microscopy coupled with energy dispersive X-ray spectroscopy and X-ray diffraction. Three three-phase regions exist in the isothermal section at 600 °C and 750 °C, respectively. The Ni–Zn phases are all in equilibrium with the liquid phase in these two isothermal sections. There is a four-phase equilibrated reaction occurred between 450 °C and 600 °C, namely β_1 + NiBi ⇔ L + α-Ni, but more experimental works are needed for obtaining the accurate equilibrated reaction temperature. Experimental results show that Bi is almost insoluble in any Ni–Zn compounds and α-Ni. The solid solubility of Zn in the NiBi phase is also limited.

1. Introduction

Hot-dip galvanizing is an effective and economic method widely used to protect steel and iron substrates from atmospheric corrosion. This technique has been in practice for over a century. Silicon is frequently introduced into steels either as deoxidant in the steel making process or as a strengthening alloy element [1]. However, silicon in steel is detrimental to the quality of hot-dip galvanizing coating. Dull grey coatings with excessive thickness will be formed when Si-containing steel are hot-dip galvanized in pure zinc bath. They are brittle and poorly adherent to the steel substrates. This phenomenon is commonly known as Si reactivity or Sandelin effect in the galvanizing industry, which has been studied extensively [2–4]. Generally, the addition of Ni into zinc bath can control the Si reactivity effectively and improve the quality of coatings [2,5,6]. Pb is another additive element in traditional galvanizing because of its beneficial effect on bath fluidity. The addition of Pb can reduce the zinc consumption and improve the 'quality-cost' ratio [7]. But the lead-bearing baths are under way to be phased out now and in the near future for environment and human health concerns. It is necessary to find an alternative of Pb. It has been reported that Bi has similar effect in hot-dip galvanizing and is taken into consideration [8–11].

Some researchers [7,12,13] have studied the synergistic effect of Ni and Bi on the microstructure of galvanized coating on the Si-containing steels. Fratesi et al. [7] reported that the addition of Ni and Bi can successfully control the Si reactivity of the Si-containing steels. On the contrary, Pedersen [12] and Pistofidis et al. [13] proposed that the addition of Ni and Bi into Zn-bath had no significant effect on the microstructure and thickness of the coatings. The phase equilibrium and thermodynamic describing of the Zn–Bi–Fe–Ni quaternary system are important to understand the combined effect of Ni and Bi in the hot-dip galvanizing. The phase relations in the Zn–Bi–Ni system at 450 °C were investigated by Liu et al. [14] using equilibrated alloys. The results showed that the L–Bi phase is in equilibrium with all phases of Ni–Zn system except the α-Ni phase, and Bi is almost insoluble in the three Ni–Zn intermetallic compounds and the α-Ni phase. In order to present a reliable basis for fine-tuned thermodynamic model of phase relations in the Zn–Bi–Fe–Ni quaternary system, in the present work, the 600 °C and 750 °C isothermal sections of the Zn–Bi–Ni system have been determined experimentally using combined techniques of optical microscopy, scanning electron microscopy-energy dispersive X-ray spectroscopy (SEM-EDS) and X-ray diffraction. The literature review that refers to three binary systems is summarized in Ref. [14].

2. Experimental methods

The phase relationship of the Zn–Bi–Ni ternary system was deduced by studying the phase makeup of the alloys. The design compositions of the alloys are listed in Tables 1 and 2 (column 2). The purity of all the starting materials is 99.99%. Samples were prepared by carefully weighing the Ni powders, Zn blocks and Bi pellets, 5 g in total for each sample. The metals of these three elements were mixed and sealed in an evacuated quartz tube. Each alloy mixture was heated to a temperature above its estimated liquidus temperature and kept at this temperature for 24 h, followed by quenching in water using a bottom-quenching technique to minimize Zn loss and reduce sample porosity. This technique has been reported elsewhere [15] and will not be detailed here. The quenched samples were resealed and annealed at 600 °C and 750 °C, respectively, for 15–20 days until an equilibrium state was reached. At the end of the treatment, all the samples were quenched in water rapidly to preserve the equilibrium state at annealing temperatures.

* Corresponding author. Tel.: +86 731 58292210; fax: +86 731 58292210.
E-mail address: fuchengyin@xtu.edu.cn (F. Yin).

0925-8388/$ – see front matter
doi:10.1016/j.jallcom.2010.06.153

Table 1
Alloy and phase compositions in the Zn–Bi–Ni ternary system at 600 °C (at.%).

No.	Design composition	Phase	Phase composition		
			Zn	Ni	Bi
A1	90Zn5Ni5Bi	L	93.1	2.1	4.8
		γ	83.8	16.2	0
A2	85Zn10Ni5Bi	L	87.5	2.4	10.1
		γ	83.3	16.7	0
A3	80Zn15Ni5Bi	L	71.3	2.4	26.3
		γ	82.1	17.9	0
A4	77.5Zn17.5Ni5Bi	L	16.8	3.4	79.8
		γ	79.7	20.3	0
A5	75Zn20Ni5Bi	L	14.9	3.4	82.7
		γ	76.7	23.3	0
A6	65Zn30Ni5Bi	L	9.7	6.1	84.2
		β_1	51.9	48.1	0
		γ	71.7	28.3	0
A7	48Zn47Ni5Bi	L	6.8	7.4	85.8
		β_1	50.9	49.1	0
A8	45Zn50Ni5Bi	L	1.6	13.4	85.0
		β_1	47.4	52.6	0
A9	32Zn48Ni20Bi	L	0	15.8	84.2
		β_1	44.2	55.8	0
		α-Ni	31.7	68.3	0
A10	15Zn55Ni30Bi	L	0	16.3	83.7
		NiBi	0	48.8	51.2
		α-Ni	29.1	70.9	0
A11	10Zn42Ni48Bi	L	0	16.5	83.5
		NiBi	0	48.7	51.3
		α-Ni	29.4	70.6	0

The samples were processed in a conventional way for microstructure examination by both optical microscopy and SEM. A nital solution was used for revealing the microstructure details of the samples. A JSM-6360LV SEM equipped with an OXFORD INCA EDS was utilized to observe the morphology and measure chemical compositions of various phases in the samples. The phase makeup of the alloys was further determined by analyzing X-ray diffraction patterns generated by a D/max-rA X-ray diffractometer with Cu Kα radiation.

Table 2
Alloy and phase compositions in the Zn–Bi–Ni ternary system at 750 °C (at.%).

No.	Designed composition	Phase	Phase composition		
			Zn	Ni	Bi
B1	80Zn15Ni5Bi	L	76.6	7.1	16.3
		γ	81.2	18.8	0
B2	73Zn22Ni5Bi	L	16.4	4.9	78.7
		γ	76.4	23.6	0
B3	70Zn25Ni5Bi	L	13.6	4.7	81.7
		γ	73.5	26.5	0
B4	67Zn28Ni5Bi	L	12.2	5.3	82.5
		γ	70.1	29.9	0
B5	60Zn35Ni5Bi	L	9.1	8.1	82.8
		γ	67.5	32.5	0
		β	54.2	45.8	0
B6	55Zn40Ni5Bi	L	9.5	7.4	83.1
		γ	67.1	32.9	0
		β	54.0	46.0	0
B7	50Zn45Ni5Bi	L	7.9	7.9	84.2
		β_1	51.3	48.7	0
		β	52.6	47.4	0
B8	45Zn50Ni5Bi	L	1.6	16.1	82.3
		β_1	46.9	53.1	0
B9	35Zn55Ni10Bi	L	1.5	19.0	79.5
		α-Ni	33.8	66.2	0
		β_1	44.3	55.7	0

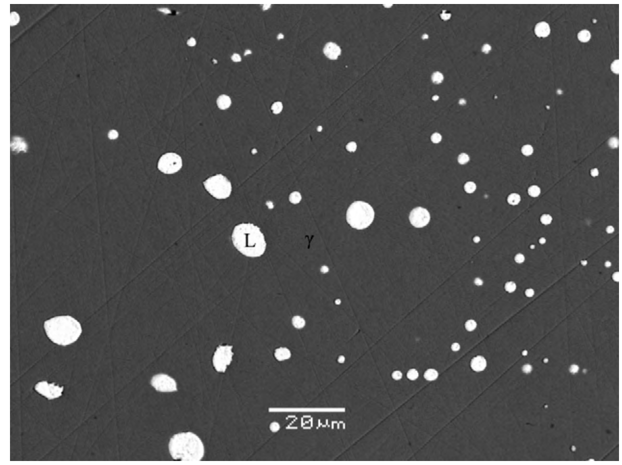

Fig. 1. The microstructure of alloy A5, which consists of two phases, L and γ.

3. Results and discussion

The phases in an alloy can easily be differentiated by studying the morphology, color, and chemical composition. In most cases, observations using SEM coupled with EDS analyses are

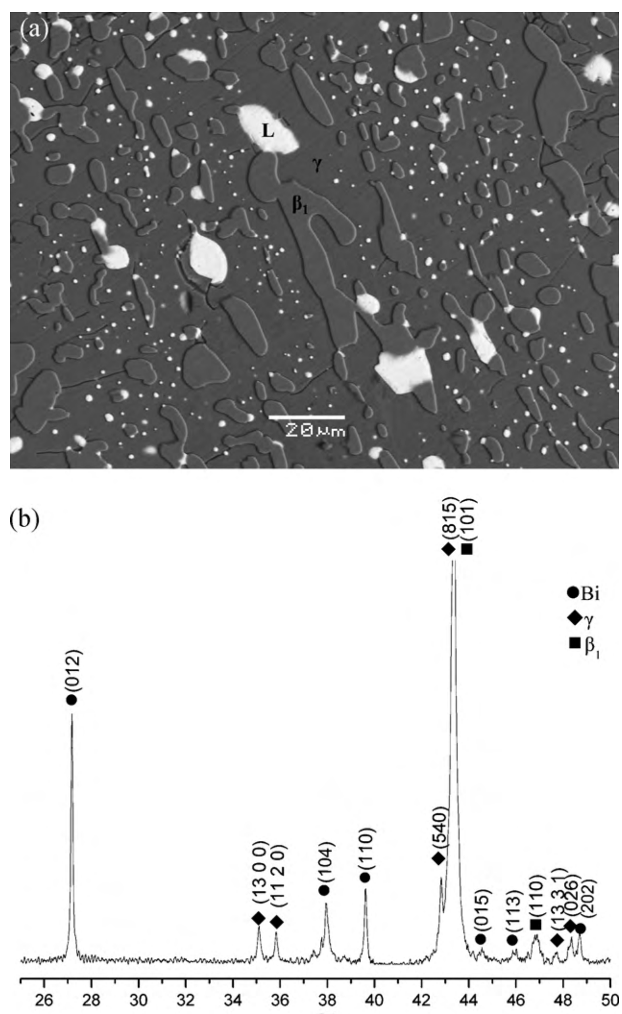

Fig. 2. The microstructure (a) and the X-ray diffraction pattern (b) of alloy A6. They indicate the γ, β_1 and L three phases coexist in this alloy.

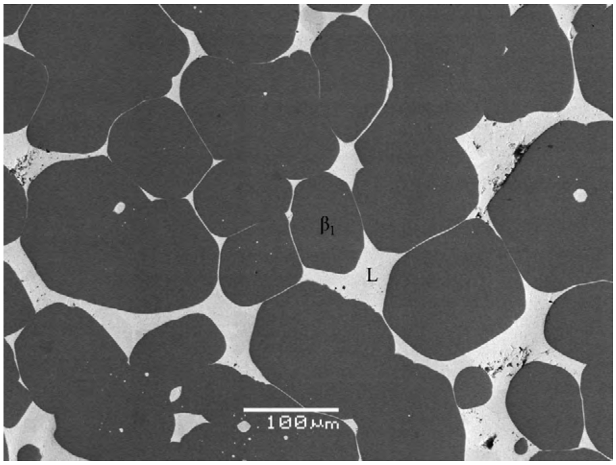

Fig. 3. The microstructure of alloy A8, which consists of L and β_1.

sufficient for phase identification. However, the relevant X-ray diffraction patterns were analyzed for the final identification of the phases. All phases confirmed in the alloys are listed in Table 1 for 600 °C and Table 2 for 750 °C (column 3), respectively, together with the chemical compositions determined by SEM-EDS. The compositions reported are the averages of at least five measurements.

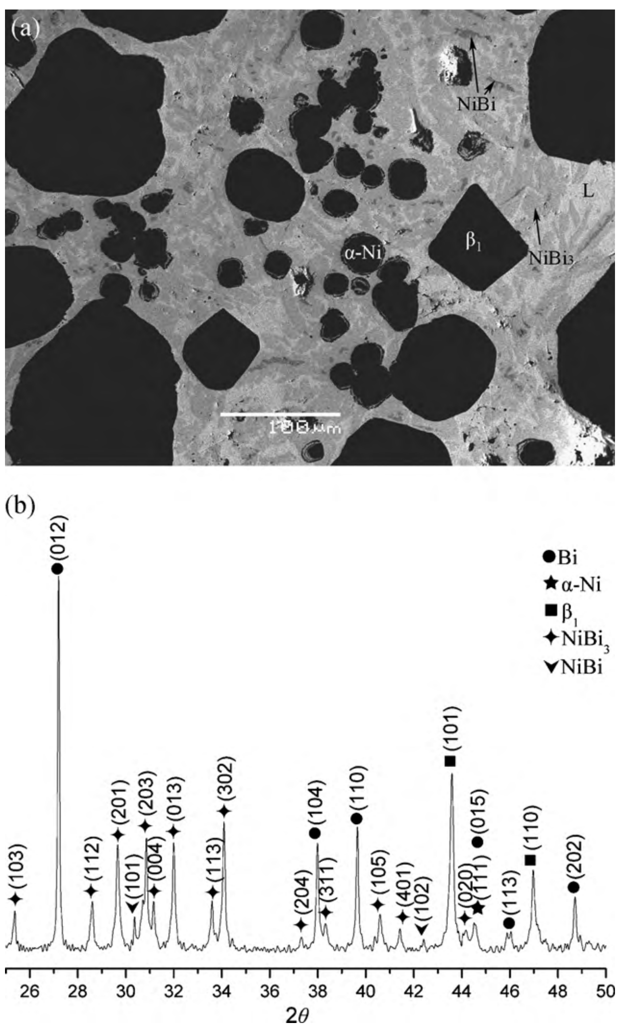

Fig. 4. The microstructure (a) and the X-ray diffraction pattern (b) of alloy A9. L, β_1, NiBi, $NiBi_3$ and α-Ni coexist in this alloy. The $NiBi_3$ and NiBi phases are formed during quenching.

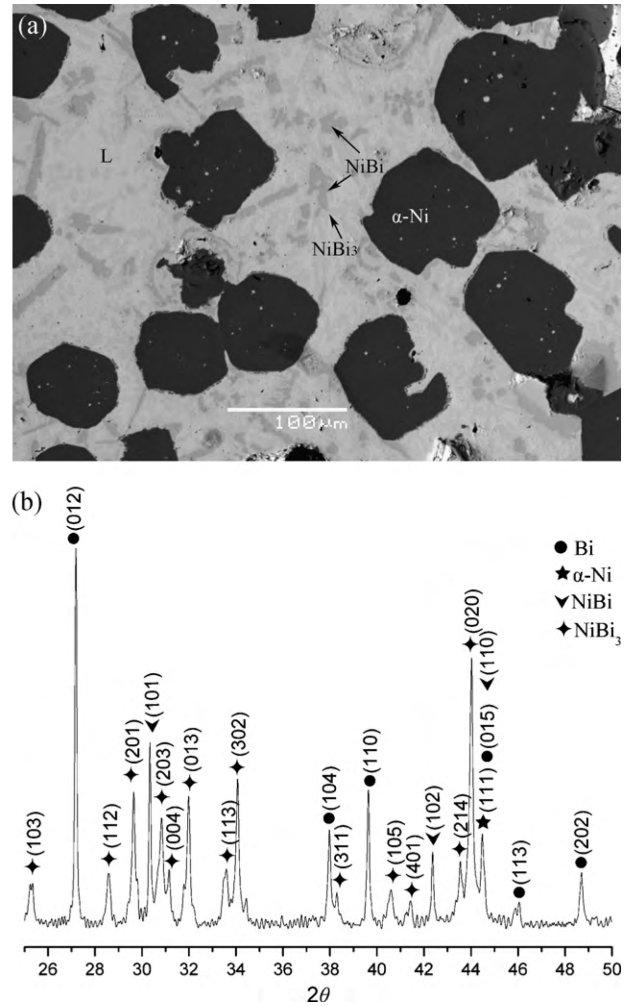

Fig. 5. The microstructure (a) and the X-ray diffraction pattern (b) of alloy A10. EDS analyses indicate that this alloy consists of four phases, namely L, NiBi, $NiBi_3$ and α-Ni. The $NiBi_3$ phase is formed during quenching.

3.1. Phase equilibria of the Zn–Bi–Ni system at 600 °C

Specimens A1–A5 were prepared based on the γ phase composition. SEM-EDS analyses of the microstructure of the specimens A1–A5 indicate that each of them consists of two phases, namely γ and L. Fig. 1 is the microstructure of A5 in which the light gray γ phase coexists with the white Bi-rich solid solution phase, marked as "L" in the figure because it is in the liquid state at 600 °C. According to the compositions of the two equilibrated phases determined by EDS, the liquidus in this two-phase region has been determined.

The microstructure of the alloy A6 is shown in Fig. 2(a). SEM-EDS analyses indicate that they are γ, β_1 and L. The gray block β_1 phase is buried in the γ phase matrix. The white L phase contains 9.7 at.% Zn and 6.1 at.% Ni. The γ and β_1 phases contain almost no Bi in solid solution. The XRD pattern of this alloy is shown in Fig. 2(b). The peaks contributed by the γ, β_1 and L phases are clearly indexed in the figure.

Specimens A7 and A8 were prepared based on the β_1 phase composition. SEM-EDS analyses indicate that each of them consists of two phases, β_1 and L. The microstructure of A8 is shown in Fig. 3. The β_1 phase contains practically no Bi. The Zn and Ni solubilities in the L phase are 6.8 at.% and 7.4 at.%, respectively.

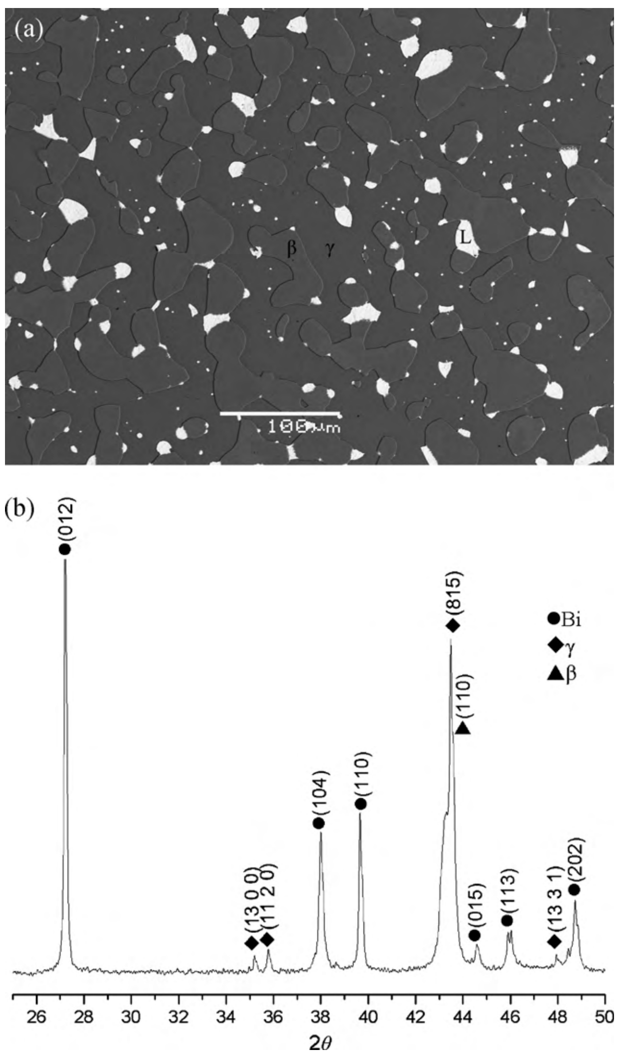

Fig. 6. The microstructure (a) and the X-ray diffraction pattern (b) of alloy B6. It is three-phase equilibrated state of the β, γ and L phases.

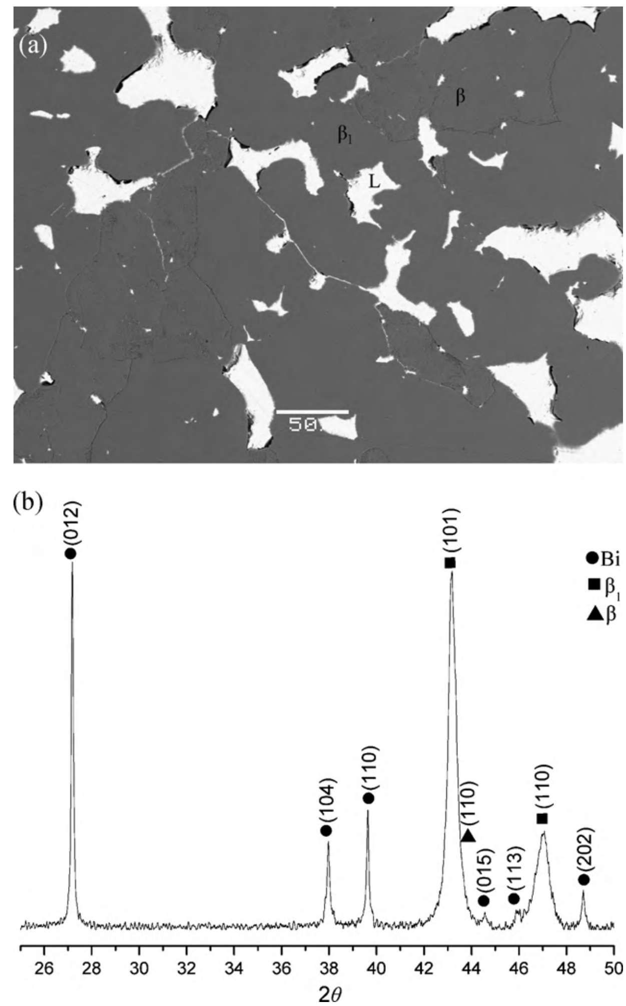

Fig. 7. The microstructure (a) and the X-ray diffraction pattern (b) of alloy B7. The β, β_1 and L three phases coexist in this alloy.

SEM-EDS analyses indicate that the alloy A9 consists of five phases. Fig. 4(a) is the microstructure of A9, in which α-Ni, β_1, NiBi, $NiBi_3$ and L coexist. The five phases can be distinguished easily by their relieves and confirmed by X-ray diffraction pattern shown in Fig. 4(b). According to the Bi–Ni binary phase diagram [16], there are two intermetallic compounds NiBi and $NiBi_3$. The $NiBi_3$ phase forms peritectically at 465 °C from the NiBi phase and the melt, the NiBi phase forms peritectically at 646 °C from the α-Ni phase and the melt. From the phase morphology, it can be deduced reasonably that the $NiBi_3$ and NiBi phases in Fig. 4(a) are formed during the quenched process. The β_1 phase contains 44.2 at.% Zn. Bi is not detected in the β_1 phase and the α-Ni phase. The EDS analyses show the average composition of the α-Ni phase is Zn31.7Ni68.3. These results are consistent with the Ni–Zn system [17].

SEM-EDS analyses indicate that the microstructure of alloy A10, shown in Fig. 5(a), corresponds to the α-Ni + NiBi + L three-phase equilibrium state. The appearance of $NiBi_3$ results from the same reason as discussed in alloy A9. With regard to the homogeneity region of the binary NiBi phase, researchers presented different results. Vassilev et al. [16] showed the composition range was 50.5–51.5 at.% Bi by EPMA, Nash [18] suggested homogeneity range as 46.5–48.3 at.% Bi. In present work, the content of Bi in the NiBi phase agrees well with the opinion of Vassilev et al., but higher than that of Nash. The X-ray diffraction pattern of A10 is shown in

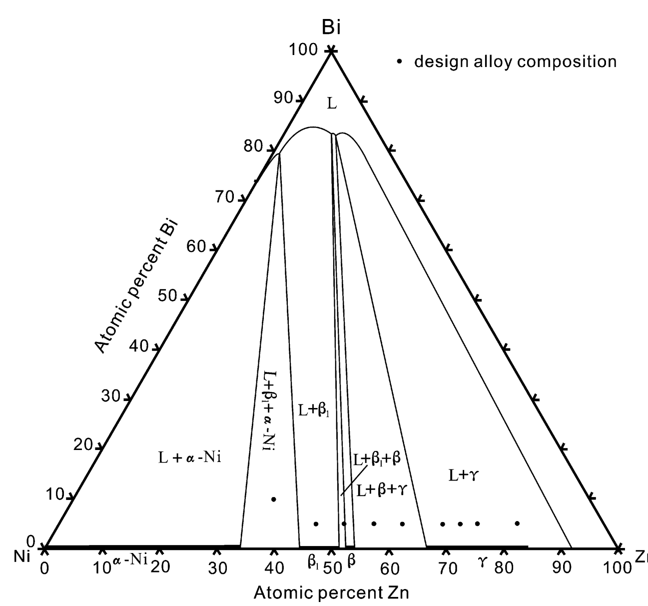

Fig. 8. The isothermal section of the Zn–Bi–Ni ternary phase diagram at 750 °C.

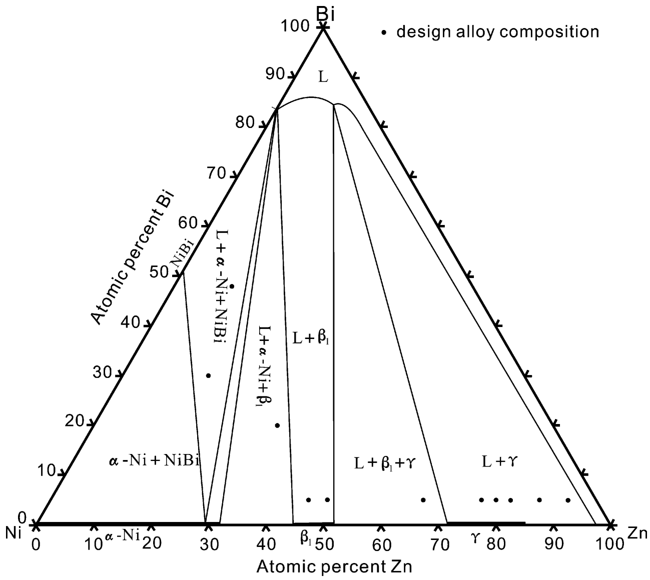

Fig. 9. The isothermal section of the Zn–Bi–Ni ternary phase diagram at 600 °C.

Fig. 5(b), which confirmed the three-phase equilibrium state. Additionally, the α-Ni + NiBi + L three-phase equilibrium state can also be found in alloy A11.

3.2. Phase equilibria of the Zn–Bi–Ni system at 750 °C

Specimens B1–B4 were prepared based on the γ phase composition. SEM-EDS analyses indicate that the microstructures of these alloys are similar, all consisting of two phases, namely γ and L. Both of alloy B5 and alloy B6 contain three phases, β, γ and L. The microstructure and X-ray diffraction pattern of B6 are shown in Fig. 6(a) and (b), respectively, which indicate that alloy B6 corresponds to the β, γ and Bi-rich L three-phase equilibrium state. The grey block β phase is buried in the γ phase matrix. The EDS results show that the average composition of the β phase is Zn54.1Ni45.9 and the γ phase is Zn67.3Ni32.7. The content of Zn in the γ phase determined in the present work is a little lower than that from the literature [16] which showed the homogeneity region of the γ phase in the Ni–Zn binary system was 72.0–85.0 at.% Zn. The white L phase contains 9.3 at.% Zn and 7.8 at.% Ni.

SEM-EDS analysis of alloy B7 reveals that the β, β_1 and L three phases coexist in this alloy. The microstructure of B7 is shown in Fig. 7(a). The relief difference between β and β_1 is obvious. The X-ray diffraction pattern of B7 can further confirm the three-phase equilibrium state of the alloy, which is shown in Fig. 7(b). The L phase contains 7.9 at.% Zn and 7.9 at.% Ni. Bi is almost insoluble in the β and β_1 phases.

Alloy B8 corresponds to the L + β_1 two-phase equilibrated state. Bi is not detected in the β_1 phase. The Zn and Ni solubilities in the L phase are 1.6 at.% and 16.1 at.%, respectively.

The coexistence of α-Ni, β_1, NiBi, $NiBi_3$ and L is found in alloy B9 by the examination of the microstructure. As discussed in alloy A9, $NiBi_3$ and NiBi in alloy B9 are formed during quenching, and alloy B9 corresponds to the L, β_1 and α-Ni three-phase equilibrated state actually. The L phase contains 1.5 at.% Zn and 19.0 at.% Ni. Bi is not detected in the β_1 phase.

Based on the experimental results, the experimental isothermal sections of the Zn–Bi–Ni ternary system at 750 °C and 600 °C are constructed in Figs. 8 and 9, respectively. There are three three-phase regions in the isothermal sections at each temperature. In these two isothermal sections, α-Ni is in equilibrium with the liquid phase, but the equilibrium is prohibited by the coexistence of NiBi and β_1 at 450 °C as shown in Fig. 10 [14]. From Fig. 8 to Fig. 10, it can be seen that the equilibrium between the liquid phase and α-Ni is changed to NiBi and β_1 coexistence state as temperature decreases. According to this, it can be deduced that there is a four-phase equilibrated reaction between 450 °C and 600 °C, namely β_1 + NiBi ⇔ L + α-Ni. But more experimental works are needed for obtaining the accurate reaction temperature. From Table 1 to Table 2, it can be seen that Bi is almost insoluble in any Ni–Zn compounds and α-Ni, and Zn is almost insoluble in NiBi.

4. Conclusion

Phase equilibria of the Zn–Bi–Ni ternary system at 600 °C and 750 °C were determined by means of SEM-EDS analyses and X-ray diffraction studies in the present work. The main results obtained are shown as follow:

1. Three three-phase regions, namely γ + β_1 + L, β_1 + α-Ni + L and NiBi + α-Ni + L, exist in the section at 600 °C, and three three-phase regions, namely β + γ + L, β + β_1 + L and β_1 + α-Ni + L, exist in the section at 750 °C.
2. There is a four-phase equilibrated reaction between 450 °C and 600 °C, namely β_1 + NiBi ⇔ L + α-Ni. But more experimental works are needed for obtaining the accurate reaction temperature.
3. The Ni–Zn compounds and α-Ni are all in equilibrium with the liquid phase in these two isothermal sections.
4. Bi is almost insoluble in any Ni–Zn compounds and α-Ni, and the solid solubility of Zn in the NiBi phase is also limited.

Acknowledgements

This investigation is supported by the Ph.D. Programs Foundation and Scientific Research Foundation of Ministry of Education of China (Nos. 20070530006 and 208094).

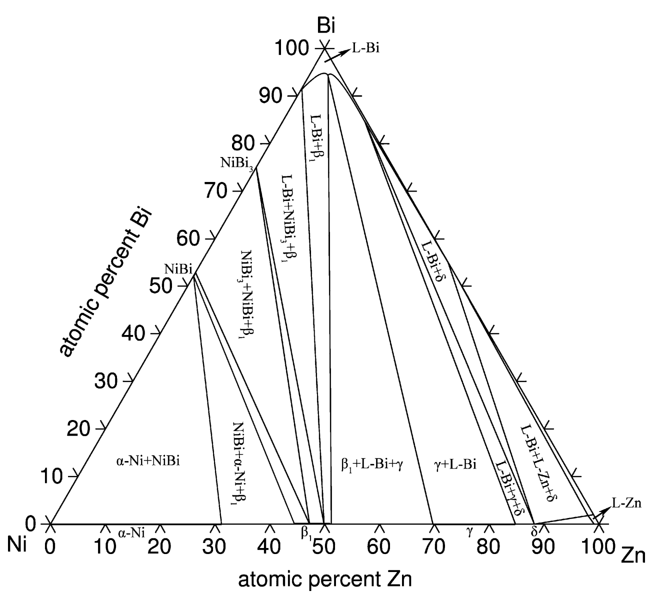

Fig. 10. The isothermal section of the Zn–Bi–Ni ternary phase diagram at 450 °C.

References

[1] N.Y. Tang, Galvatech 04 Conference Proceedings, Chicago, USA, 2004, p. 683.
[2] R.W. Sandelin, Wire Wire Prod. 15 (1940) 3.
[3] X.P. Su, N.Y. Tang, J. Phase Equilib. 23 (2002) 424.
[4] J. Foct, P. Perrot, G. Reumont, Scripta Metall. Mater. 28 (1993) 1195.

[5] J. Foct, G. Reumont, P. Perrot, in: A.R. Marder (Ed.), The Physical Metallurgy of Zn Coated Steel, TMS, Warrendale, PA, 1993, p. 1.
[6] F.C. Porter, A.M. Stonemen, R.G. Thicthorph, Trans. IMF 66 (1988) 28.
[7] R. Fratesi, N. Ruffini, M. Malavolta, T. Bellezze, Surf. Coat. Technol. 157 (2002) 34.
[8] K.C.D. Judd, S.J. White, F. Akbari, J.R. Mcdermid, W.T. Thompson, Can. Metall. Q 45 (1) (2006) 117.
[9] N. Moelans, K.C. Hari Kumar, P. Wollants, J. Alloys Compd. 360 (2003) 98.
[10] M Gagnĭe, Proceedings of 18th International Galvanizing Conference EGGA, Birmingham (UK), 1997.
[11] M. Gagnĭe, US Patent 5,445,791.
[12] J. Pedersen, Fourth Asia Pacific General Galvanizing Conference, Kuala Lumpur, 1999.
[13] N. Pistofidis, G. Vourlias, S. Konidaris, El. Pavlidou, A. Stergiou, G. Stergioudis, Mater. Lett. 61 (2007) 994.
[14] Y.X. Liu, F.C. Yin, H. Tu, Z. Li, J.H. Wang, X.P. Su, J. Phase Equilib. Diff. 29 (2008) 493.
[15] X.P. Su, N.Y. Tang, J.M. Toguri, Can. Metall. Q 40 (2001) 377.
[16] G.P. Vassilev, X.J. Liu, K. Ishida, J. Phase Equilib. 26 (2005) 161.
[17] X.P. Su, N.Y. Tang, J.M. Toguri, J. Phase Equilib. 23 (2002) 140.
[18] P. Nash, in: T.B. Massalski (Ed.), Binary Alloy Phase Diagrams, 2nd, ASM, 1990, p. 768.